MAGNETIC RESONANCE IN CHEMISTRY
Magn. Reson. Chem. 2006; **44**: 241–248
Published online in Wiley InterScience (www.interscience.wiley.com). DOI: 10.1002/mrc.1756

MRC

Molecular reorientation of CD_4 in gas-phase mixtures†

Marc A. ter Horst,[1] Cynthia J. Jameson[2]* and A. Keith Jameson[3]

[1] Department of Chemistry, University of North Carolina at Chapel Hill, Venable and Kenan Laboratories, Chapel Hill, North Carolina 27599, USA
[2] Department of Chemistry, University of Illinois at Chicago, Chicago Illinois 60607, USA
[3] Emeritus Department of Chemistry, Loyola University, Chicago Illinois 60626, USA

Received 23 September 2005; Revised 24 October 2005; Accepted 26 October 2005

Spin-lattice relaxation times were measured for the deuterons in CD_4 in pure gas and in mixtures with the following buffer gases: Ar, Kr, Xe, HCl, N_2, CO, CO_2, CF_4, and SF_6. Effective collision cross sections $\sigma_{\theta,2}$ for the molecular reorientation of CD_4 in collisions with these ten molecules are obtained as a function of temperature. These cross sections are compared with the corresponding cross sections σ_J obtained from ^1H spin-rotation relaxation in mixtures of CH_4 with the same set of buffer gases. Various classical reorientation models typically applied in liquids predict different ratios of the reduced correlation times for the reorientation of spherical tops. The Langevin model comes closest to predicting the magnitude of the $\sigma_{\theta,2}/\sigma_J$ ratio that we obtain for CD_4. Copyright © 2006 John Wiley & Sons, Ltd.

KEYWORDS: NMR; ^2H; gas phase; relaxation; CD_4; molecular reorientation

INTRODUCTION

In dilute gases of polyatomic molecules, the phenomena that are directly related to the anisotropy of the intermolecular potential function include angular momentum alignment phenomena and the effects of collisions on radiation absorption or scattering. Kinetic theory allows each of these properties to be described in terms of an effective cross section that can be calculated if the intermolecular potential function is known.[1,2] Of the angular momentum alignment phenomena, nuclear spin relaxation in the gas phase offers the possibility of exploring the same potential surface with more than one probe nucleus, thus providing either redundant or additional information. Spin relaxation due to interactions of unlike pairs of molecules can be characterized nearly as precisely as relaxation owing to collisions between like molecules in contrast with other thermophysical properties. Furthermore, the factors that relate the effective cross section to the spin relaxation times are well defined, and unambiguous, with no associated normalization problems. The relaxation times associated with specific relaxation mechanisms can involve first or second rank irreducible tensors; they can be related directly to a specific effective cross section for changes in the molecular angular momentum vector. The relaxation cross sections are determined by the anisotropic part of the intermolecular potential and can be obtained via scattering theory.[3,4] McCourt and coworkers provide a detailed derivation of the collision cross sections related to various thermophysical properties, including nuclear magnetic resonance spin relaxation.[1,2] A particular type of cross section that can be derived from NMR experiments is associated with the quadrupolar, dipole–dipole, and chemical shift anisotropy mechanisms. This cross section is closely related to (for atomic collision partners, is identical to) the cross section that can be derived from depolarized Rayleigh light scattering. Another type of cross section, associated with the spin-rotation relaxation mechanism, can only be obtained from NMR relaxation and is known to be an independent probe of the anisotropy of the potential energy surface (PES). In fact, even with structural information and vibrational spectroscopy of the van der Waals complex, the PES cannot be adequately specified without some anisotropy information farther up from the bottom of the well. This is the type of information that spin relaxation cross sections provide.[5,6] Together, these cross sections have been found very useful in refining the anisotropy of intermolecular potential functions for H_2 with He,[7–11] HD and D_2 with He,[12] H_2 with Ne,[13] H_2 with Ar,[14–16] D_2 and HD with Ar,[17,18] CO_2 with Ar,[19] N_2 with Ar,[5,20,21] N_2 with Kr,[6,22] and N_2 with N_2.[23] Intermolecular potential functions, particularly for unlike pairs of molecules, are of interest in their own right and have many applications.

In favorable systems, effective cross sections can be obtained directly from relaxation times T_1 measured in the gas phase.[24–32] Having obtained the cross sections for spin-rotation relaxation for ^1H in the CH_4 molecule in the presence of ten collision partners,[29] we now report here the quadrupolar relaxation of ^2H in CD_4 with the same set of ten collision partners in order to obtain the other type of relaxation cross section.

†Dedicated to Professor David M. Grant of the University of Utah on the occasion of his 75th birthday, in recognition of the outstanding contributions he has made to the methodology of nuclear magnetic resonance and its application to a wide range of chemical topics over a long period of time.

*Correspondence to: Cynthia J. Jameson, Department of Chemistry, University of Illinois at Chicago, Chicago IL 60607, USA.
E-mail: cjjames@uic.edu
Contract/grant sponsor: National Science Foundation;
Contract/grant number: CHE-9979259.

Despite the fact that methane is a simple molecule, the intermolecular potentials involving CH_4 with itself or with rare gas atoms and simple molecules are not accurate enough to reliably predict the thermophysical properties of gas mixtures, beam scattering data, and intermolecular effects on spectra, including rotational and vibrational dynamics of van der Waals complexes.[33] Recent work has focused primarily on CH_4–Ar and CH_4–CH_4 potential surfaces and indicate some of the difficulties associated with determining potential functions for even these cases.[34–36] Therefore, the availability of spin relaxation cross sections for the CD_4 molecule in collisions with the set of molecules we have used will encourage the detailed examination of the PES for these molecules.

An interesting application of the relaxation times of the type reported here is to the adsorption of molecules in porous materials. The methane molecule has been used as a probe to examine various porous materials using NMR as well as other techniques. Of particular interest is the application of CH_4 as a probe of zeolites, and zeotype materials such as $ALPO_4$-5, $ALPO_4$-11, SAPO-11, and MCM-41.[37–39] In these cages and channels, methane is used to study the effects of confinement on the chemical shift tensor of the ^{13}C, on phase transitions, transport, molecular mobility, and separation from gas mixtures. Intercalation of CD_4 into crystalline C_{60} has been studied.[40] The authors measured the ^2H relaxation time and found that $T_1 = 17.9 \pm 1.8$ s at 213–300 K and they suggest that this is an indication that CD_4 rotates freely while intercalated into crystalline C_{60}. It is not possible to deduce the latter from the measured relaxation time without making comparisons with T_1 in other CD_4 environments. In contrast, our experiments reveal that the $^2HT_1$ relaxation times for CD_4 occluded in the cages of zeolite NaA are dependent on occupancy, temperature, and magnetic field.[41] In all cases, the relaxation times of the occluded CD_4 are longer than those of free CD_4 in the overhead gas. Relaxation measurements on CD_4 in the overhead gas provide internal consistency with respect to dependence on magnetic field and temperature in addition to providing a quantitative measure of overhead gas density. The molecular reorientation of the CD_4 molecule will be significantly different in confined geometries such as pores, cages, or channels in comparison to the bulk gas phase. Therefore, the measured relaxation times can provide a test of the dynamical behavior of CD_4 inside the cavity, which in turn depends on the potential energy the CD_4 molecule experiences under the combined influence of the atoms of the cavity wall, which in turn depends on cavity size and shape, as well as the electronic nature of the atoms that make up the walls. The advantage of using the ^2H relaxation of CD_4 as a probe of internal surfaces is that, given a potential function to test, the molecular dynamics simulation of the reorientation of the CD_4 molecules inside the pores leads to the evaluation of the autocorrelation function $\langle P_1[u(0)\cdot u(t)]\rangle/\langle P_1[u(0)\cdot u(0)]\rangle$ as a function of time, the Fourier transform of which provides $\Im(\omega) = \int_{-\infty}^{+\infty}\langle P_2[u(0)\cdot u(t)]\rangle/\langle P_2[u(0)\cdot u(0)]\rangle \exp^{-i\omega t}\,dt$ from which the quadrupolar relaxation rate can be expressed as,[42]

$$\left(T_1^{Q}\right)^{-1} = \frac{3}{80}\left(\frac{e^2qQ}{\hbar}\right)^2 [\Im(\omega_0) + 4\Im(2\omega_0)] \qquad (1)$$

and compared with the measurements. This is fairly straightforward for CD_4 since the largest component of the electric field gradient tensor lies along the C–D bond and the description of CD_4 motion as a rigid rotor should suffice; the molecule does not require consideration of internal rotations or torsions. There have been many molecular dynamics simulations of methane in zeolite cavities. Examples of recent work include the use of methane as a model probe of cylindrical pores; orientational preference and influence of rotation on molecular mobility and pore–pore correlation effects have been investigated, as well as transport diffusivities of methane in CH_4-CF_4 mixtures in a zeolite.[43–46]

The spin-lattice relaxation times that we report here can be used for refinement of intermolecular potential functions involving methane and for applications utilizing CH_4 or CD_4 as a probe of molecular crystals, porous, and amorphous materials.

EXPERIMENTAL

The gas samples were prepared by condensing a known amount of the gas into a 4 mm × 5 cm glass tube held in a liquid nitrogen bath. The tubes were then sealed off from the vacuum line with a torch and placed in an oven maintained at about 450 K to ensure the integrity of the samples throughout the temperature range of the T_1 measurements. These tubes just fit into a 5 mm NMR tube. The buffer gases used were Ar, Kr, Xe, N_2, HCl, CO, CO_2, CH_4, CF_4, and SF_6; all were used as obtained from vendors. Gas densities ranged from 7 to 50 amagat (1 amagat is defined as the number density in an ideal gas at standard conditions, i.e. 2.687×10^{19} molecules cm^{-3}) and the nitrogen densities were corrected for uncondensed gas at liquid nitrogen temperature. The estimated error in the densities of N_2 is 4% and in the other gases is about 2–3%.

Spin-lattice relaxation times were measured using the inversion recovery pulse sequence (the magnetization is inverted with a π pulse, spins are allowed to relax for some delay time τ_D and is sampled to the degree of recovery to equilibrium with a $\pi/2$). The system is allowed to relax to equilibrium, waiting $\sim 5T_1$ before the sequence is repeated. Seven variable delay times, ranging from 0.2 to about 1.8 T_1, were used in shuffled order so as to minimize systematic errors. The delay times τ_0 and τ_∞ were added to the beginning and end of the delay list for an independent check of the stability of experimental conditions. The shortest delay time allowed by the spectrometer (0.3 μs) was used for τ_0 and a value equal to or greater than 5 T_1 was used for τ_∞. The delay list was cycled through a number of times for more reliable averages over any variations in conditions over time. The experiments were run unlocked and the field was shimmed on the ^1H FID of a methanol or ethylene glycol sample used for temperature determination. The temperature of the sample was determined absolutely to within ±0.5 K and was regulated to better than 0.1 K. Plots of $\ln[(A_\infty - A_D)/(A_\infty - A_0)]$ vs τ_D provide a slope $-1/T_1$. Condensation of HCl, CO_2, Xe, and SF_6 in the samples containing mixtures of CD_4 with these buffer gases set a lower limit on the temperature range, which could be used

to obtain relaxation times for the corresponding CD_4–X interactions. All others were studied in the range 200–400 K.

RESULTS

For nuclei with spin >1/2 in gas-phase molecules, the quadrupolar relaxation rate is almost always the largest. When this rate is significantly larger than the other rates, the smaller rates can be neglected and the analysis becomes straightforward. We have found that ^1H relaxation in CH_4 in gas mixtures is dominated by the spin-rotation mechanism, and the dipole–dipole mechanism is not very large.[29] Thus, nuclear spin-lattice relaxation times measured for ^2H relaxation in the CD_4 molecule in mixtures of CD_4 in buffer gases were analyzed in terms of the spin-rotation and quadrupolar mechanisms only.

$$R_1(\text{observed}) = R_1(\text{Q}) + R_1(\text{SR}) \tag{2}$$

where

$$R_1 = {T_1}^{-1}$$

The rates for each of the two mechanisms were determined from equations of the form

$$R_1 = \left[\left(\frac{T_1}{\rho}\right)_{\text{CD}_4-\text{CD}_4} \cdot \rho_{\text{CD}_4} + \left(\frac{T_1}{\rho}\right)_{\text{CD}_4-\text{X}} \cdot \rho_X\right]^{-1} \tag{3}$$

since the measured relaxation times are in the extreme narrowing limit, where the relaxation time is directly proportional to density ρ (the linear regime). In order to extract the desired $(T_1/\rho)^{\text{Q}}_{\text{CD}_4-\text{X}}$ for each CD_4-buffer combination, independent measures of $(T_1/\rho)^{\text{SR}}_{\text{CD}_4-\text{CD}_4}$, $(T_1/\rho)^{\text{SR}}_{\text{CD}_4-\text{X}}$, and $(T_1/\rho)^{\text{Q}}_{\text{CD}_4-\text{CD}_4}$ are needed. To obtain the spin-rotation $(T_1/\rho)^{\text{SR}}_{\text{CD}_4-\text{CD}_4}$ and $(T_1/\rho)^{\text{SR}}_{\text{CD}_4-\text{X}}$, we use the spin-rotation value of $(T_1/\rho)_{^2\text{H}}$, which has been derived from the spin-rotation value of $(T_1/\rho)_{^1\text{H}}$ from the earlier ^1H relaxation studies in CH_4 gas mixtures[29] using scaling factors we have previously derived to take into account the mass dependence of the various factors that enter into spin-rotation relaxation[47] as follows:

$$\left(\frac{T_1}{\rho}\right)^{\text{SR}}_{^2\text{H}} = \left(\frac{T_1}{\rho}\right)^{\text{SR}}_{^1\text{H}} \times \frac{{B_0}^{(\text{D})}}{{B_0}^{(\text{H})}} \times \left(\frac{{g_\text{N}}^{(\text{H})}}{{g_\text{N}}^{(\text{D})}}\right)^2 \times \left(\frac{\mu^{(\text{H})}}{\mu^{(\text{D})}}\right)^{1/2} \times \frac{{y_{ij}}^{(\text{H})}}{{y_{ij}}^{(\text{D})}} \tag{4}$$

Here the notation on each molecular property corresponds to the molecular species involving the proton (H), whereas the (D) corresponds to the species involving the deuteron. B_0 is the rotational constant of the molecule, g_N is the g value of the nucleus, μ is the reduced mass corresponding to the CH_4-buffer pair or the CD_4-buffer pair, and y_{ij} are the kinematic factors defined in Ref. 47:

$$y_{ij} = \left[\frac{2I_i}{\mu_{ij}{d_{ii}}^2} + \frac{1}{2}\left(1 + \frac{{d_{jj}}^2 I_i}{{d_{ii}}^2 I_j}\right)\right]^{-1} \tag{5}$$

where ij corresponds to the CH_4-buffer pair or the CD_4-buffer pair. Here I is the moment of inertia, d is the hard sphere diameter for the corresponding molecule in the pair, and μ_{ij} is the reduced mass of the collision complex. Previous relaxation measurement studies for ^1H in CH_4 in the same set of buffer gases provide the spin-rotation relaxation rate appropriate for CH_4 with each buffer gas. For ^2H in CD_4, the spin-rotation mechanism is found to comprise an average of 7% of the total relaxation rate and ranges from 6 to 8% for individual buffer gases.

Table 1 lists the values obtained from the analysis of the remainder that is attributed to the quadrupolar relaxation in terms of Eqn (3). Within the density ranges used (7–37 amagat), the quadrupolar relaxation time constants, ${T_1}^{\text{Q}}$, varied linearly with the density of the constituent gases and the temperature dependence according to the same simple power law used for the ^{14}N relaxation in the N_2 and NNO systems.

$$\left(\frac{T_1}{\rho}\right)_T = \left(\frac{T_1}{\rho}\right)_{300\text{ K}} \cdot \left(\frac{T}{300}\right)^n \tag{6}$$

The errors quoted are taken from the standard deviations of $(T_1/\rho)_{300\text{ K}}$ and n in the plot of $\ln(T_1/\rho)$ vs $\ln(T/300)$ for all measurements in all samples for each collision partner. Figure 1 shows such a plot for pure CD_4. The results in Table 1 may have a greater degree of uncertainty than is indicated by the quoted standard deviations owing to systematic errors associated with imperfect subtraction of the spin-rotation contribution.

In a previous study of deuterium relaxation in CD_4 in various condensed phase systems, Beckmann *et al*. also measured relaxation times in low density (0.1–5.5 atmospheres) CD_4 gas.[48] Their 0.1 atm sample shows a T_1 below that which would be predicted from a linear dependence on the density of the other samples. It was argued that this discrepancy was due to the influence of centrifugal distortion splittings that are the same order of magnitude as the Larmor frequency of the deuterium nucleus. The authors did not explicitly consider contributions to other mechanisms such as spin-rotation although they did observe a linear pressure

Table 1. Quadrupolar relaxation times for ^2H in CD_4 with various collision partners. The observed temperature dependence can be described by (T_1/ρ) [T], ms amagat^{-1} = (T_1/ρ)[300 K] × $(T/300\text{ K})^n$[a]

Collision partner	(T_1/ρ)[300 K], ms amagat^{-1}	n
CD_4	77.2 ± 3.4	−0.15 ± 0.03
N_2	71.5 ± 1.3	−0.10 ± 0.03
CO	69.9 ± 1.4	−0.08 ± 0.03
Ar	60.7 ± 1.2	−0.15 ± 0.02
HCl	93.0 ± 1.5	−0.09 ± 0.03
CO_2	100.8 ± 1.7	−0.21 ± 0.03
CF_4	95.2 ± 3.1	−0.16 ± 0.03
Kr	71.4 ± 2.2	−0.17 ± 0.03
Xe	77.8 ± 1.8	−0.25 ± 0.03
SF_6	115.6 ± 1.7	−0.06 ± 0.03

[a] Temperature ranges are 215–400 K for CD_4 in CD_4, Ar, CF_4; 230–400 K for CD_4 in Kr, N_2, CO; 265–400 K for CD_4 in Xe, CO_2; 280–400 K for CD_4 in HCl; 290–400 K for CD_4 in SF_6.

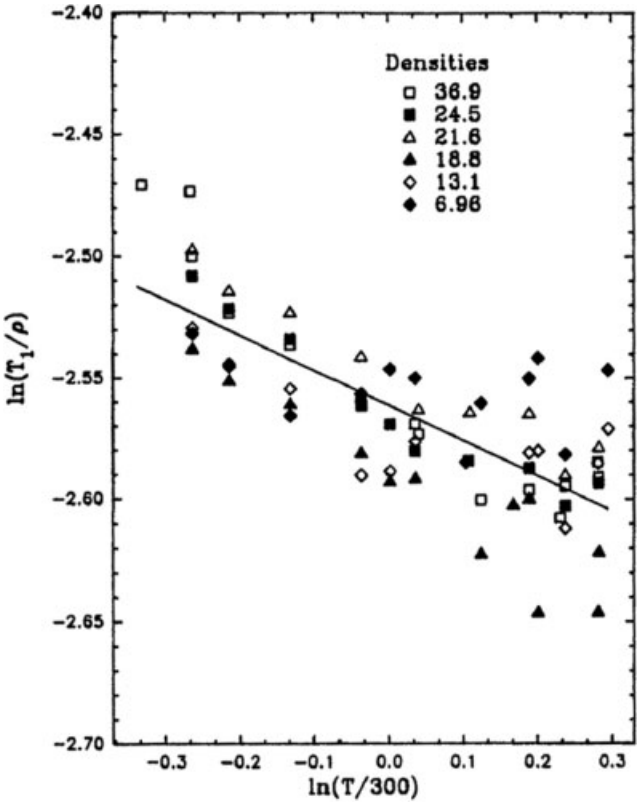

Figure 1. Temperature dependence of (T_1/ρ) for ^{2}H relaxation in pure CD_4 gas.

dependence for the higher density gas samples, indicating the dominance of a single relaxation mechanism. The effects from centrifugal splittings were not observed for densities greater than 0.5 amagat. The densities of the samples used in the present study range from 7 to 37 amagat for the CD_4 gas samples, so this effect is not expected to contribute to ^{2}H relaxation in CD_4 in our work.

Values for the quadrupolar cross section $\sigma_{\theta,2}$ were calculated using the value for the coupling constant $e^2qQ/\hbar = 191.48 \pm 0.77$ kHz,[49] in the equation that applies to the extreme narrowing limit,[50]

$$\left(T_1^{Q}\right)^{-1} = \frac{3}{40}\frac{(2I+3)}{I^2(2I-1)}\left(\frac{e^2qQ}{\hbar}\right)^2\left\langle\frac{j^2}{4j^2-3}\right\rangle\frac{1}{\rho\langle v\rangle\sigma_{\theta,2}} \quad (7)$$

where the mean relative speed is $\langle v\rangle = (8k_BT/\pi\mu)^{1/2}$. Since the spin precession in the magnetic field is slow compared to molecular rotation frequencies, only the conserved or rotationally averaged component of the intramolecular magnetic field, modulated by collisions, contributes to the relaxation. In gases, spin relaxation depends on the changes produced by collisions in a quantity (the electric field gradient tensor in this case) averaged over the free rotational motion between collisions.[1,2,50]

The average $\langle j^2/4j^2-3\rangle$ or $\langle J(J+1)/(2J-1)(2J+3)\rangle$ approaches 1/5 for spherical top molecules such as CD_4, except at extremely low temperatures. We therefore take 1/5 as our average for this quantity.

$$T_1^{Q} = \frac{200}{3}\frac{I^2(2I-1)}{(2I+3)}\left(\frac{\hbar}{e^2qQ}\right)^2\rho\langle v\rangle\sigma_{\theta,2} \quad (8)$$

In this treatment, we use the high-temperature limit, which is valid for the range of temperatures used in this study. At very low temperatures, it would be necessary, among other things, to separately consider ortho and para spin states and the limitations on the rotational states they are associated with in keeping with the Pauli exclusion principle.

The same power law is used to describe the temperature dependence of the quadrupolar relaxation cross section,

$$(\sigma_{\theta,2})_T = (\sigma_{\theta,2})_{300\ K}\cdot\left(\frac{T}{300}\right)^m \quad (9)$$

where $m = n - 0.5$, in which the 0.5 arises from the explicit temperature dependence of the mean relative speed. The values of $(\sigma_{\theta,2})_{300\ K}$ are listed in Table 2 along with the standard deviations. The cross sections are plotted as a function of temperature in Figs 2, 3, and 4.

DISCUSSION

Trends in the cross sections

As can be seen in Table 2, the values for the cross sections $\sigma_{\theta,2}$(300 K) tend to increase with the size of the collision partner in a series, such as Ar, Kr, Xe; CO, CO_2; CD_4, CF_4, SF_6. Values for CD_4-SF_6 are largest among the collision pairs. This was also found to be the case for NNO-SF_6.[32] Relaxation times for all pairs have a negative power dependence on temperature. The temperature dependence follows a similar trend with size, but not uniformly so. The change of $\sigma_{\theta,2}$(300 K)

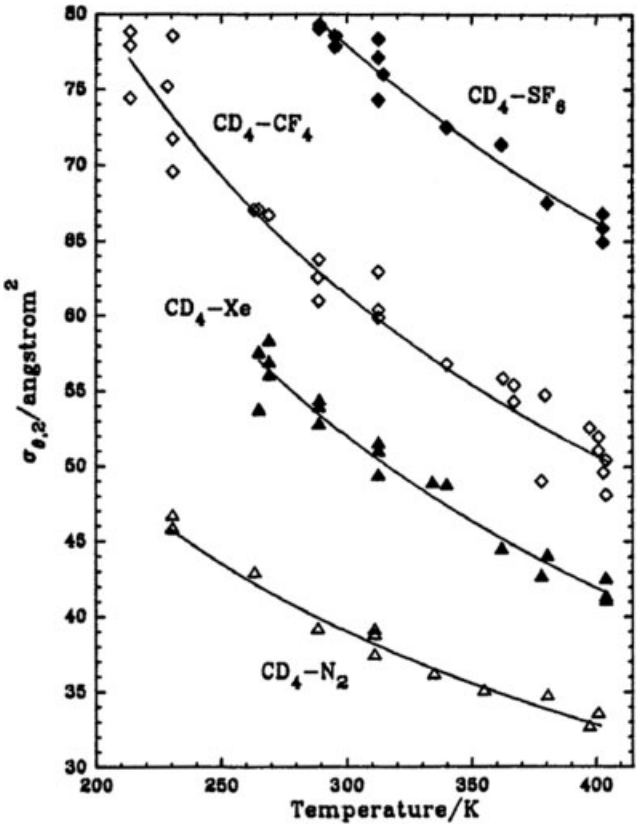

Figure 2. The quadrupolar relaxation cross section $\sigma_{\theta,2}$ for the CD_4 molecule in collisions with N_2, Xe, CF_4, and SF_6 molecules.

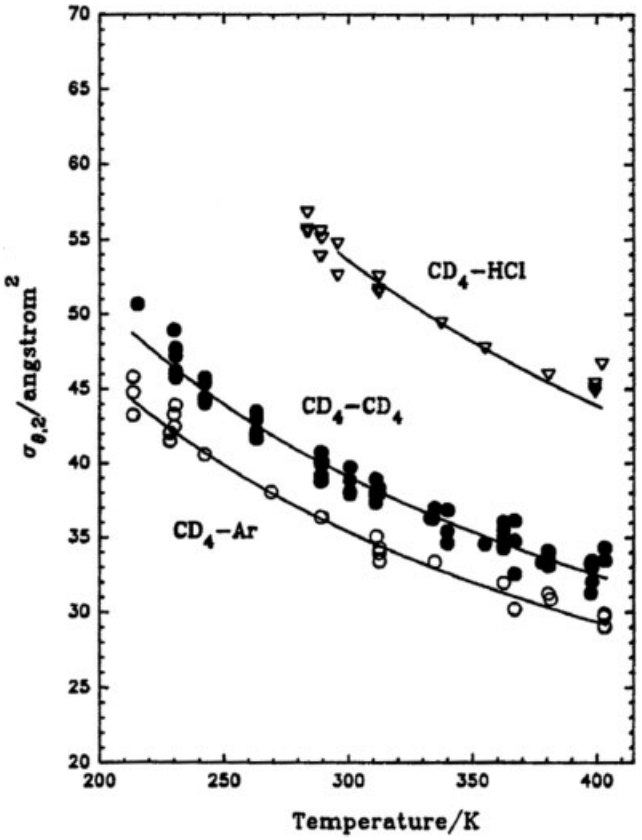

Figure 3. The quadrupolar relaxation cross section $\sigma_{\theta,2}$ for the CD_4 molecule in collisions with Ar, CD_4, and HCl molecules.

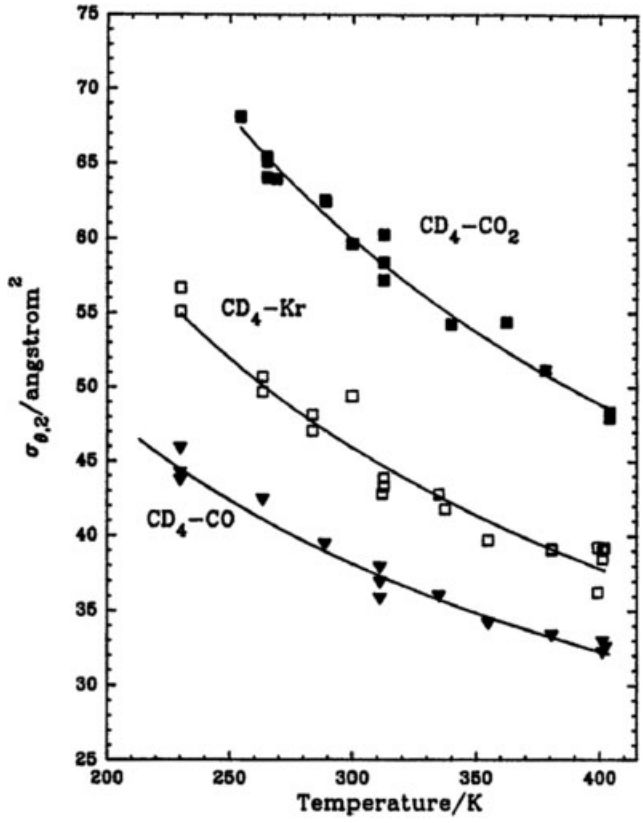

Figure 4. The quadrupolar relaxation cross section $\sigma_{\theta,2}$ for the CD_4 molecule in collisions with CO, Kr, and CO_2 molecules.

along the CD_4, CF_4, SF_6 sequence is not systematic. The CD_4-buffer $\sigma_{\theta,2}$ cross sections have a temperature dependence that is less pronounced than that of the corresponding σ_J. The $\sigma_{\theta,2}$ cross sections do not appear to have systematic trends of the temperature dependence with increasing contributions to the interaction energy from the electric moments (e.g. dipole, quadrupole) or with the polarizability of the buffer molecule, with the possible exception of Xe. A very clear trend is that the temperature dependence of the $\sigma_{\theta,2}$ cross sections for CD_4-buffer combinations is systematically less than those found for the analogous NNO-buffers,[32] or the N_2-buffers.[31] Such a trend with respect to the probe molecule may be indicative of a dependence of m on the anisotropic part of the relevant PES; the linear molecules have greater anisotropy of structure than the spherical top.

To properly compare the relative magnitudes of the cross sections for various interaction pairs, we consider the collision efficiencies, $(\sigma_{\theta,2}/\sigma_{\text{geom}})$, which permit comparisons while taking into account the size differences among the collision partners. Here, the geometric cross section σ_{geom} is taken to be πr_0^2, where r_0 is the average distance at which

Table 2. Relaxation cross sections (Å^2) for the rotational angular momentum vector in the CD_4 molecule with various collision partners. The temperature dependence can be described by $\sigma[T] = \sigma[300\text{ K}] \times (T/300\text{ K})^m$

	This work		a		
Collision Partner	$\sigma_{\theta,2}$[300 K], Å^2	m	σ_J[300 K], Å^2	m	Ratio $\sigma_{\theta,2}/\sigma_J$
CD_4	39.1 ± 1.7	-0.65 ± 0.03	18.4 ± 0.4	-0.90 ± 0.03	2.1
N_2	39.0 ± 0.7	-0.60 ± 0.03	16.3 ± 0.3	-0.87 ± 0.03	2.4
CO	38.1 ± 0.7	-0.58 ± 0.03	15.8 ± 0.2	-0.83 ± 0.02	2.4
Ar	35.4 ± 0.7	-0.65 ± 0.02	14.4 ± 0.5	-0.79 ± 0.05	2.5
HCl	53.6 ± 0.9	-0.59 ± 0.03	23.7 ± 0.4	-0.90 ± 0.06	2.3
CO_2	59.9 ± 1.1	-0.71 ± 0.03	24.1 ± 1.0	-0.98 ± 0.10	2.5
CF_4	61.4 ± 2.0	-0.66 ± 0.03	24.4 ± 0.7	-0.80 ± 0.04	2.5
Kr	45.9 ± 1.4	-0.67 ± 0.04	18.3 ± 0.6	-0.87 ± 0.04	2.5
Xe	52.0 ± 1.2	-0.75 ± 0.04	22.4 ± 0.2	-1.06 ± 0.02	2.3
SF_6	77.9 ± 1.2	-0.56 ± 0.03	34.5 ± 1.1	-0.82 ± 0.08	2.3

[a] On the basis of ^{1}H relaxation in CH_4-X pairs from Ref. 29.

Table 3. Collision efficiencies at 300 K for changes in the rotational angular momentum vector of the CD_4 molecule with various collision partners

Collision partner	σ_{geom}[a]	$\sigma_{\theta,2}/\sigma_{geom}$	σ_J/σ_{geom}
CD_4	43.49	0.90	0.42
N_2	41.44	0.94	0.39
CO	40.53	0.94	0.39
Ar	35.26	1.00	0.41
HCl	35.03	1.53	0.68
CO_2	44.63	1.34	0.54
CF_4	65.87	0.93	0.37
Kr	40.29	1.14	0.45
Xe	48.20	1.08	0.46
SF_6	86.66	0.90	0.40

[a] The geometric cross section is defined as $\sigma_{geom} = \pi r_0^2$, where r_0 values were taken as arithmetic means of the r_0 for like pairs. The latter were taken from the pair potentials on the basis of corresponding states, from Ref. 51, except for r_0(CO–CO) = 3.592 Å (Ref. 52) and r_0(HCl–HCl) = 3.3349 Å (Ref. 53).

the isotropic average potential function is zero. The r_0 values were taken as arithmetic means of the r_0 for like pairs. The latter were taken from the pair potentials on the basis of corresponding states, from Ref. 51, except for r_0(CO–CO) = 3.592 Å[52] and r_0(HCl–HCl) = 3.3349 Å.[53] Table 3 lists the collision efficiencies ($\sigma_{\theta,2}/\sigma_{geom}$) for CD_4-buffer combinations, and these are compared with the collision efficiencies (σ_J/σ_{geom}) found for CD_4-buffers. It is evident that when the implicit dependence of the cross section on the size of the collision partner is taken into account by comparing collision efficiencies rather than cross sections, HCl stands out as having a larger collision efficiency than all the others, with CO_2 being the next largest. These larger values appear to be related to the attractive potential arising from the large dipole moment of the HCl molecule and the large electric quadrupole of the CO_2 molecule. As collision partners, Ar, Kr, and Xe become more similar when collision efficiencies are compared rather than cross sections. The efficiencies do not follow a systematic trend with respect to the electric dipole polarizability of the collision partner. This is to be expected; since the first nonvanishing permanent electric moment of CD_4 is the octopole moment, induction contributions to the intermolecular interaction are smaller than for NNO or for CO, for example.

The ratio of the two types of cross sections, ($\sigma_{\theta,2}/\sigma_J$), can provide some insight into the differences and similarities of the two cross sections. The ratios of the cross sections are shown in Table 2; they range from 2.3 to 2.5 except for CD_4 itself, for which it is 2.1. This is a very narrow range, unlike the 0.96–1.67 range that was found for NNO-X with the same set of buffer molecules.[32]

Comparison with reorientation models

In a dilute gas, the cross sections $\sigma_{\theta,2}$ and σ_J can be calculated from first principles.[2] On the other hand, the complexity of intermolecular interactions prohibits a simple description of the dynamics in the liquid phase. The persistence of a molecular rotational angular momentum is not as unambiguous in the liquid as in the dilute gas. Nevertheless, for a given molecule in a fluid, the correlation times τ_J, $\tau_{\theta,1}$, and $\tau_{\theta,2}$ are related to each other by the nature of the reorientation model used to describe the motion of molecules in a liquid. The reduced correlation times τ_J^*, $\tau_{\theta,1}^*$, and $\tau_{\theta,2}^*$ are defined as follows:

$$\tau_J^* = \left(\frac{k_B T}{I_0}\right)^{1/2} \int \frac{\langle J(0)\cdot J(t)\rangle}{\langle J(0)\cdot J(0)\rangle} dt \quad (10a)$$

$$\tau_{\theta,1}^* = \left(\frac{k_B T}{I_0}\right)^{1/2} \int \frac{\langle P_1[u(0)\cdot u(t)]\rangle}{\langle P_1[u(0)\cdot u(0)]\rangle} dt \quad (10b)$$

$$\tau_{\theta,2}^* = \left(\frac{k_B T}{I_0}\right)^{1/2} \int \frac{\langle P_2[u(0)\cdot u(t)]\rangle}{\langle P_2[u(0)\cdot u(0)]\rangle} dt \quad (10c)$$

where $(k_B T/I_0)^{1/2}$ is the average time for a classical rotor, in thermal equilibrium at temperature T, to rotate by an angle of one radian. In the liquid phase, where $\tau_J^* << 1$, all the various reorientation models (the extended diffusion model,[54] Ivanov model,[55,56] Langevin model,[57] and friction model[58]) predict $(\tau_{\theta,2}^*/\tau_J^*) = 1/6$, which agrees with the Hubbard relation,[59] as predicted by Debye's rotational diffusion model that provides an accurate description of molecular reorientation in dense fluids at low temperatures.[60] On the other hand, Powles and Rickayzen[61] have shown that the various models can be distinguished from one another when $\tau_J^* >> 1$. In particular, they demonstrated that in the limit of very large τ_J^* (in the dilute gas), the ratio of the reduced correlation times for the reorientation of spherical tops approaches different values,

$$\lim \tau_{J\to\infty}^* \left(\frac{\tau_{\theta,2}^*}{\tau_J^*}\right) = \frac{5}{4} \text{ for the Ivanov model}$$
$$= \frac{1}{4} \text{ for the extended diffusion model}$$
$$= \frac{1}{24.4} \ldots \text{for the Langevin model} \quad (11)$$

For spherical tops, the friction model predicts a constant value of 5.14 for $\tau_{\theta,2}^*$, independent of τ_J^*. For our gas-phase data, the appropriate quantity to compare with the $\tau_{\theta,2}^*$ of the various models is the $1/[5\rho\langle v\rangle\sigma_{\theta,2}]$, where the factor 1/5 is the numerical factor derived by Bloom *et al.* for spherical tops in dilute gases with free rotation between collisions; only the rotationally averaged component of the electric field gradient tensor contributes to relaxation.[62] Both the classical average $\langle j^2/4j^2-3\rangle$ and the quantum average $\langle J(J+1)/(2J-1)(2J+3)\rangle$ approach 1/5 for spherical top molecules. Thus, these reorientation models provide the following expected values for the cross section ratio for spherical tops in the gas phase: $(\sigma_{\theta,2}/\sigma_J) = 0.25$ for the Ivanov model, 0.8 for the extended diffusion model, and 4.88 for the Langevin model. Instead, we found the experimental ratios of cross sections to be clustered very closely around 2.4.

Figure 5 shows the relationship between the NMR experimental results and the predictions of the models. The τ_J^* results for CD_4-X were obtained from scaling the results of the relaxation cross sections for ^1H in CH_4 to ^2H in CD_4,

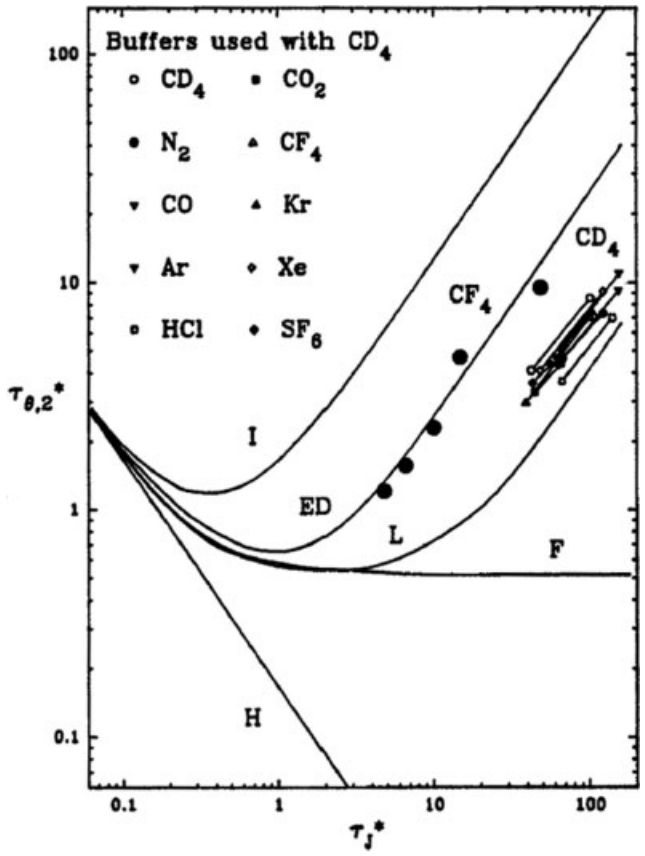

Figure 5. Comparison of the correlation times for CD_4 in various gas mixtures against predictions of various models for molecular reorientation. Included also are CF_4 correlation times for comparison. The labels corresponding to the various reorientation models are I = Ivanov, ED = extended diffusion, L = Langevin, F = friction model. In the liquid phase, where $\tau_J* << 1$, all models predict $(\tau^*_{\theta,2}/\tau^*_J) = 1/6$, which agrees with the Hubbard relation (labeled H).

as already discussed under the section on 'Results'. Thus, our gas-phase results fall between the extended diffusion model and the Langevin model, lying somewhat closer to the Langevin model. Also shown are the results from ^{19}F relaxation experiments on CF_4.[63] For CF_4, the extended diffusion model agrees very well with experiment.

CONCLUSIONS

This is the first report of the $\sigma_{\theta,2}$ relaxation cross sections for CD_4 determined from NMR spin relaxation measurements as a function of temperature for a variety of CD_4-X systems. The contribution of the spin-rotation to the overall relaxation rate is about 8%, derived from measurements of ^1H T_1 relaxation in analogous CH_4-X mixtures. Comparison of $\sigma_{\theta,2}$ to σ_J values shows that the ratios $\sigma_{\theta,2}/\sigma_J$ are 2.3–2.5 (except for CD_4 itself), relatively insensitive to the nature of the various collision partners. This is in contrast to N_2-X pairs and NNO-X pairs for which the ratio is close to 2.1 and 1.3, respectively, with somewhat greater variability. This clearly indicates the overwhelming importance of the nature of the probe molecule for these relaxation cross sections. The temperature-dependent CD_4-X and CH_4-X cross sections reported here can be used to refine PESs for interaction of CD_4 or CH_4 with these ten collision partners when trial potential functions are used in classical trajectory calculations of various thermophysical properties, including these two types of relaxation cross sections. We have previously demonstrated that the relaxation cross sections provide good discrimination between proposed intermolecular potential functions for N_2-X, CO_2-X and NNO-X where X = rare gas.[6,19,22,64] Comparison with the results of various reorientation models for spherical tops in liquids favor the Langevin model, the only model for which the ratio $\tau^*_J/\tau^*_{\theta,2}$ is greater than 1. The spin-lattice relaxation times that we report here can be used for applications utilizing CH_4 or CD_4 as a probe of internal spaces in molecular crystals, porous, and amorphous materials.

Acknowledgements

This research was supported by the National Science Foundation (Grant CHE-9979259).

REFERENCES

1. McCourt FRW, Beenakker JJM, Kohler WE, Kuščer I. *Nonequilibrium Phenomena in Polyatomic Gases. Part I. The Dilute Gas*, vol. 1. Oxford University Press: Oxford, 1990.
2. McCourt FRW, Beenakker JJM, Kohler WE, Kuščer I. *Nonequilibrium Phenomena in Polyatomic Gases. Part II. Cross Sections, Scattering and Rarefied Gases*, vol. 2. Oxford University Press: Oxford, 1990.
3. Nielsen WB, Gordon RG. *J. Chem. Phys.* 1973; **58**: 4131.
4. Nielsen WB, Gordon RG. *J. Chem. Phys.* 1973; **58**: 4149.
5. Beneventi L, Casavecchia P, Volpi GG, Wong CCK, McCourt FRW. *J. Chem. Phys.* 1993; **98**: 7926.
6. ter Horst MA, Jameson CJ. *J. Chem. Phys.* 1995; **102**: 4431.
7. Lemaire C, Armstrong RL, McCourt FRW. *J. Chem. Phys.* 1984; **81**: 5275.
8. Armstrong RL, Bogdan M, Jeffrey KR, Bissonnette C, McCourt FRW. *J. Chem. Phys.* 1993; **99**: 5754.
9. Wagner RS, Armstrong RL, Bissonnette C, McCourt FRW. *J. Chem. Phys.* 1990; **92**: 5907.
10. Lazarides AA, Rabitz H, McCourt FRW. *J. Chem. Phys.* 1994; **101**: 4735.
11. McCourt FRW, Weir D, Clark GB, Thachuk M. *Mol. Phys.* 2005; **103**: 17.
12. McCourt FRW, Weir D, Thachuk M, Clark GB. *Mol. Phys.* 2005; **103**: 45.
13. Wagner RS, Armstrong RL, Lemaire C, McCourt FRW. *J. Chem. Phys.* 1986; **84**: 1137.
14. Lemaire C, McCourt FRW. *Can. J. Phys.* 1985; **63**: 179.
15. Lemaire C, Armstrong RL, McCourt FRW. *J. Chem. Phys.* 1987; **87**: 6499.
16. Sabzyan H, McCourt FRW, Power WP. *J. Chem. Phys.* 2004; **120**: 4306.
17. Sabzyan H, Power WP, McCourt FRW. *J. Chem. Phys.* 1998; **108**: 2361.
18. Sabzyan H, Power WP, McCourt FRW. *J. Chem. Phys.* 1998; **108**: 6170.
19. ter Horst MA, Jameson CJ. *J. Chem. Phys.* 1996; **105**: 6787.
20. Dham AK, McCourt FRW, Meath WJ. *J. Chem. Phys.* 1995; **103**: 8477.
21. Jäger W, Gerry MCL, Bissonnette C, McCourt FRW. *Faraday Discuss. Chem. Soc.* 1994; **97**: 105.
22. McCourt FRW, ter Horst MA, Jameson CJ. *J. Chem. Phys.* 1995; **102**: 5752.
23. Cappelletti D, Vecchiocattivi F, Pirani F, Heck EL, Dickinson AS. *Mol. Phys.* 1998; **93**: 485.

24. Jameson CJ, Jameson AK, Buchi K. *J. Chem. Phys.* 1986; **85**: 697.
25. Jameson CJ, Smith NC, Jackowski K. *J. Chem. Phys.* 1987; **86**: 2717.
26. Jameson CJ, Jameson AK, Smith NC. *J. Chem. Phys.* 1987; **86**: 6833.
27. Jameson CJ, Jameson AK. *J. Chem. Phys.* 1988; **88**: 7448.
28. Jameson CJ, Jameson AK. *J. Chem. Phys.* 1988; **89**: 866.
29. Jameson CJ, Jameson AK, Smith NC, Hwang JK, Zia T. *J. Phys. Chem.* 1991; **95**: 1092.
30. Jameson CJ, Jameson AK, Terry R. *J. Phys. Chem.* 1991; **95**: 2982.
31. Jameson CJ, Jameson AK, ter Horst MA. *J. Chem. Phys.* 1991; **95**: 5799.
32. Jameson CJ, ter Horst MA, Jameson AK. *J. Chem. Phys.* 1998; **109**: 10 227.
33. Wormer PES, van der Avoird A. *Chem. Rev.* 2000; **100**: 4109.
34. Geleijns M, Wormer PES, van der Avoird A. *J. Chem. Phys.* 2002; **117**: 7551.
35. Hayes JM, Greer JC, Morton-Blake DA. *J. Comput. Chem.* 2004; **25**: 1953.
36. Johnson ER, Wolkow RA, DiLabio GA. *Chem. Phys. Lett.* 2004; **394**: 334.
37. Coulomb JP, Floquet N, Martin C, Kahn R. *Eur. Phys. J.* 2003; **12**: S25.
38. Koskela T, Ylihautala M, Vaara J, Jokisaari J. *Chem. Phys. Lett.* 1996; **261**: 425.
39. Koskela T, Ylihautala M, Jokisaari J, Vaara J. *Phys. Rev., B* 1998; **58**: 14 833.
40. Morosin B, Assink RA, Dunn RG, Massis TM, Schirber JE, Kwei GH. *Phys. Rev., B* 1997; **56**: 13 611.
41. Jameson CJ, Baello BI to be published.
42. Abragam A. *The Principles of Nuclear Magnetism*. Clarendon Press: Oxford, 1961.
43. Radhakrishnan R, Gubbins KE. *Phys. Rev. Lett.* 1997; **79**: 2847.
44. Bhide SY, Yashonath S. *J. Chem. Phys.* 2002; **116**: 2175.
45. Papadopoulos GK. *Mol. Simul.* 2005; **31**: 57.
46. Skoulidas AI, Sholl DS, Krishna R. *Langmuir* 2003; **107**: 10 132.
47. Jameson CJ, Jameson AK. *J. Chem. Phys.* 1990; **93**: 3237.
48. Beckman P, Bloom M, Burnell EE. *J. Chem. Phys.* 1986; **84**: 5898.
49. Wofsy SC, Muenter JS, Klemperer W. *J. Chem. Phys.* 1970; **53**: 4005.
50. Gordon RG. *J. Chem. Phys.* 1965; **44**: 228.
51. Maitland GC, Rigby M, Smith EB, Wakeham WA. *Intermolecular Forces: Their Origin and Determination*. Clarendon Press: Oxford, 1981.
52. Trengove RD, Robjohns JL, Dunlop PJ. *Ber. Bunsen-Ges. Phys. Chem.* 1984; **88**: 450.
53. Turfa AF, Marcus RA. *J. Chem. Phys.* 1979; **70**: 3035.
54. Gordon RG. *J. Chem. Phys.* 1966; **44**: 1830.
55. Ivanov EN. *Sov. Phys. JETP* 1964; **18**: 1041.
56. Kluk E. *Mol. Phys.* 1975; **30**: 1723.
57. McConnell J. *The Theory of Nuclear Relaxation in Liquids*. Cambridge University Press: New York, 1987.
58. Kluk E, Powles JG. *Mol. Phys.* 1975; **30**: 1109.
59. Hubbard PS. *Phys. Rev.* 1963; **9**: 481.
60. McClung RED. *J. Chem. Phys.* 1969; **51**: 3842.
61. Powles JG, Rickayzen G. *Mol. Phys.* 1977; **33**: 1207.
62. Bloom M, Bridges F, Hardy WN. *Can. J. Phys.* 1967; **45**: 3533.
63. Campbell JH, Seymour SJ, Jonas J. *J. Chem. Phys.* 1973; **59**: 4151.
64. ter Horst MA, Jameson CJ. *J. Chem. Phys.* 1998; **109**: 10 238.